

## Simultaneous step meandering and bunching instabilities controlled by Ehrlich-Schwoebel barrier and elastic interaction

Yan-Mei Yu, Axel Voigt, Xiaoshu Guo, and Yong Liu

Citation: *Appl. Phys. Lett.* **99**, 263106 (2011); doi: 10.1063/1.3666781

View online: <http://dx.doi.org/10.1063/1.3666781>

View Table of Contents: <http://apl.aip.org/resource/1/APPLAB/v99/i26>

Published by the [American Institute of Physics](http://www.aip.org).

---

### Related Articles

Density functional theory simulations of amorphous high-oxides on a compound semiconductor alloy: a-Al<sub>2</sub>O<sub>3</sub>/InGaAs(100)-(4×2), a-HfO<sub>2</sub>/InGaAs(100)-(4×2), and a-ZrO<sub>2</sub>/InGaAs(100)-(4×2)  
*J. Chem. Phys.* **135**, 244705 (2011)

Structural and electrical characterization of silicided Ni/Au contacts formed at low temperature (<300°C) on p-type [001] silicon  
*J. Appl. Phys.* **110**, 123510 (2011)

Preface to Special Topic: Selected Papers from The Eleventh International Conference on Surface X-Ray and Neutron Scattering  
*J. Appl. Phys.* **110**, 102101 (2011)

Shape transition and migration of TiSi<sub>2</sub> nanostructures embedded in a Si matrix  
*J. Appl. Phys.* **110**, 094304 (2011)

First-principles study of the spin-mixing conductance in Pt/Ni<sub>81</sub>Fe<sub>19</sub> junctions  
*Appl. Phys. Lett.* **99**, 172105 (2011)

---

### Additional information on *Appl. Phys. Lett.*

Journal Homepage: <http://apl.aip.org/>

Journal Information: [http://apl.aip.org/about/about\\_the\\_journal](http://apl.aip.org/about/about_the_journal)

Top downloads: [http://apl.aip.org/features/most\\_downloaded](http://apl.aip.org/features/most_downloaded)

Information for Authors: <http://apl.aip.org/authors>

### ADVERTISEMENT

The logo for AIP Advances features the text 'AIP Advances' in a blue and green font. Above the text is a decorative graphic of several orange and yellow circles of varying sizes, arranged in a curved path that suggests motion or a trail.

*Submit Now*

Explore AIP's new  
open-access journal

- Article-level metrics now available
- Join the conversation! Rate & comment on articles

# Simultaneous step meandering and bunching instabilities controlled by Ehrlich-Schwoebel barrier and elastic interaction

Yan-Mei Yu,<sup>1,a)</sup> Axel Voigt,<sup>2,a)</sup> Xiaoshu Guo,<sup>3</sup> and Yong Liu<sup>3</sup>

<sup>1</sup>*Institute of Physics, Chinese Academy of Science, P.O. Box 603, 100080 Beijing, China and Beijing National Laboratory of Condensed Matter Physics, Beijing 100190, China*

<sup>2</sup>*Institut für Wissenschaftliches Rechnen, Technische Universität Dresden, 01062 Dresden, Germany*

<sup>3</sup>*Department of Applied Physics, Yanshan University, Qinhuangdao 066004, China*

(Received 7 September 2011; accepted 17 November 2011; published online 29 December 2011)

Through phase-field simulations, we investigate simultaneous step meandering and bunching instabilities with the presence of Ehrlich-Schwoebel barrier and elastic interaction. The meandering instability induced by the Ehrlich-Schwoebel barrier is found to be dependent on the elastic interaction at low adatom deposition rate. The ordered step meandering-bunching structure is designed by using the predefined magnitude distribution of the force monopoles on vicinal surfaces based on interplay between the Ehrlich-Schwoebel barrier and the elastic interaction. © 2011 American Institute of Physics. [doi:10.1063/1.3666781]

During growth, a uniform vicinal surface is known to undergo two types of primary instabilities: step meandering (SM) and step bunching (SB), which has become an important topic in nanoscience research from the fundamental thermodynamics of surfaces to the fabrication of surface nanostructures.<sup>1,2</sup> Taking advantage of the deterministic instabilities to monitor vicinal surfaces and using them as a template for nanostructure formation is one promising issue. One possible direction is to use templates which simultaneously undergo bunching and meandering instabilities, leading to a two dimensional pattern. The bunching-meandering morphology has been observed on the Cu vicinal surfaces.<sup>3</sup> However, the meandering-bunching structure with long-range order, which is required for application in nanoscience, has not been obtained yet in experiments. In order to reaching a mature level toward application, a more refined understanding of interplay between various physical ingredients that drive the meandering and bunching instabilities is needed.

The step instability may be caused by many different driving forces. For instance, the Ehrlich-Schwoebel (ES) barrier causes an asymmetric adatom incorporation rate at steps, driving in-phase step meandering (phase shift of two steps is zero).<sup>4-6</sup> In the case of heteroepitaxy, elasticity drives out-of-phase step meandering (phase shift of two steps is  $\pi$ ) and step bunching.<sup>7-10</sup> The linear stability analysis has predicted crossover from out-of-phase SM to SB on vicinal surfaces under stress but with the ES barrier absent.<sup>9</sup> Another linear stability analysis has predicted transformation between in-phase SM and out-of-phase SM due to competition of the ES barrier and the elastic interaction.<sup>10</sup> These results indicate two different instability modes could coexist due to compromise between different instability driving forces on the vicinal substrate when initial step separation (average distance between two steps) is of a critical value at the intermediate state.

In this paper, we reproduce the simultaneous instability of SM and SB with the presence of the strain and the ES barrier by using the phase-field model. We use the deposition rate as a controlling parameter for transformation between two instability modes instead of the step separation. The SM instability induced by the ES barrier vanishes at small deposition rates when the stress is absent. However, under the same condition of such small deposition rates, when the ES barrier and the stress effect both are incorporated, the ES-barrier-driven SM instability remains prominent and coexists with the stress-driven SB instability. The results indicate interplay of the ES barrier, and the elastic effect is evoked under the small deposition rates. The interplay role of the ES barrier and the elastic interaction might affect the critical value of the initial step separation of the vicinal substrate for transformation between two instability modes. Further, we design a hybrid meandering-bunching structure by using predefined magnitude distribution of the force monopoles on the vicinal surface.

The system to be solved reads

$$\partial_t \phi = \frac{1}{\tau} \left[ \nabla \cdot (W(\vartheta)^2 \nabla \phi) - 2 \sin(2\pi\phi) - 2\lambda(\cos(2\pi\phi) - 1)u + \frac{1}{2}P \frac{\partial v_i}{\partial x_i} - \frac{1}{2}Q \frac{\partial^2 v_i}{\partial x_i^2} \right], \quad (1)$$

$$\partial_t u = \nabla \cdot (D \nabla u) - \partial_t \phi + F, \quad (2)$$

where  $\phi$  is the phase-field variable, taking values of 0, 1, 2, 3, ...,  $n$  corresponding to the substrate and the first, second, third, ..., and the  $n$ th monolayer (ML);  $u$  is the adatom density-field variable;  $v_i$  with  $i=1,2$  represents the elastic displacement in the horizontal and vertical directions. The step energy anisotropy enters the system through  $W(\vartheta) = W_0 a_s(\vartheta)$ , where  $\vartheta$  is the angle of the step normal direction with respect to the horizon<sup>11,12</sup>; the elastic monopole-monopole interaction (EMMI) and the elastic dipole-dipole interaction (EDDI) enter through  $P \partial v_i / \partial x_i$  and  $Q \partial^2 v_i / \partial x_i^2$ , respectively, wherein  $P$  and  $Q$  are magnitudes of the force

<sup>a)</sup>Authors to whom correspondence should be addressed. Electronic addresses: ymyu@aphy.iphy.ac.cn and axel.voigt@tu-dresden.de.

monopole and dipole,  $x_i$  with  $i=1,2$  represents the horizontal and vertical coordinations, where the summation over subscript  $i$  is implicit;<sup>13–15</sup> the diffusion rate  $D$  equals to  $D_0$  on the terrace but reduces to  $D_{es}$  in the thin zone of phase-field transition at the step in order to imitate the ES effect, where  $D_0 = v \exp(-E_d/k_B T)$ ,  $D_{es} = D_0 \exp(-E_s/k_B T)$ ,  $v$  is attempt frequency,  $E_d$  is diffusion barrier,  $E_s$  is ES barrier,  $k_B$  is Boltzmann constant, and  $T$  is temperature.<sup>11,12</sup> The displacement field is calculated using the surface elastic Green function.<sup>13–15</sup>

Equations (1) and (2) are solved on a uniform grid of size  $200\Delta x \times 200\Delta x$  with the grid space  $\Delta x=1$ , where the length is rescaled by the atomic lattice constant  $a$ , and the time stepping  $\Delta t < \Delta x^2/5D_0$  is required. The vicinal substrate is defined as  $\phi_0 = \text{int}[(l_0 + y)/l_0]$  with initial step separation  $l_0 = 12\Delta x$ , and  $y$  is grid node in the horizontal direction. The periodic boundary conditions are used for  $(\phi - \phi_0)$  and  $u$ . We choose  $W=2$ ,  $\lambda=0.36W/d_0$  with the capillary length  $d_0=1.8 \times 10^{-4}$ ,  $\tau=0.51W^2\lambda/D_0$  (fast atomic attachment at steps is assumed),  $D_0$  and  $D_{es}$  are determined by  $E_d=0.40$  eV,  $E_s=0.052$  eV,  $v=10^{12}$ , and  $T=250$  K referring to MBE growth conditions for Cu(001) vicinal surfaces. We use  $a_s(\vartheta) = 1 + \eta \cos 4\vartheta$  with  $\eta=0.07$  for the step energy anisotropy. Unless stated otherwise,  $P=1$  for the case of EMMI, and  $Q=1$  for the case of EDDI. The height of the film grown above the vicinal substrate is defined as  $h(\vec{r}) = (\phi - y/l_0)$ . The root-mean-square (RMS) roughness  $w$  of the height of the grown film (hereafter called as surface roughness) is defined as  $w = \langle (h(\vec{r}) - \langle h \rangle)^2 \rangle$ . In the case of film growth of the step instability,  $w$  tends to increase with time usually, corresponding to the surface roughening process. The simulation results are visualized by the surface plot of  $h(\vec{r})$ , as shown in Figs. 1 and 2.

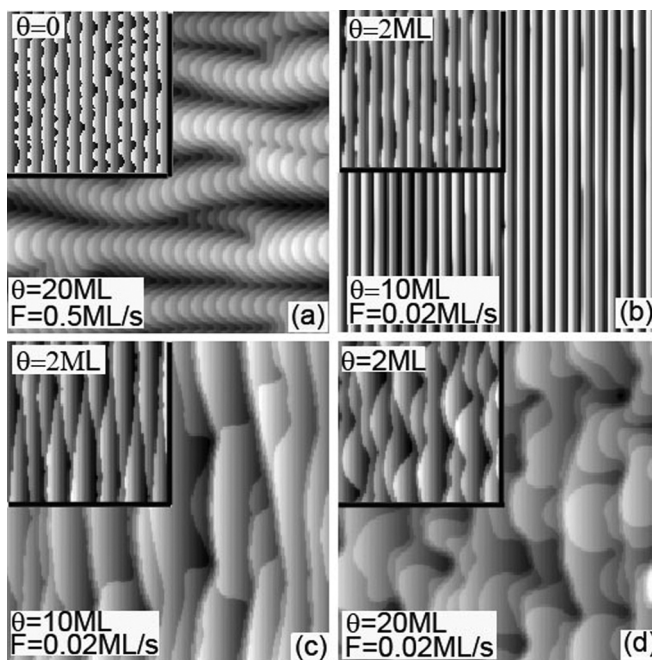


FIG. 1. Simulated step morphologies: in-phase SM (a) and stable step-flow (b) with the presence of ES barrier for different deposition rates  $F$ ; out-of-phase SM (inset of (c)) and SB (c) with the presence of EMMI; simultaneous SM and SB with the presence of ES barrier and EMMI. Inset of (a) is initial step profile that is used for all our simulations.

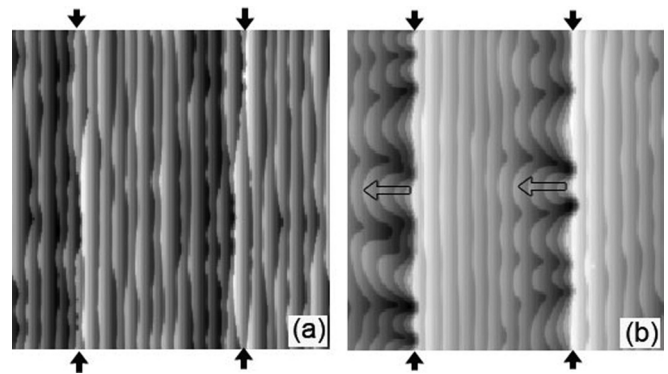


FIG. 2. Simulated step morphologies: (a) locally, SB (denoted by solid arrows) directed by predefined EMMI; (b) in-phase SM proceeds (in the direction marked by open arrows) ahead of SB under the predefined EMMI and ES barrier.

The ES-barrier-driven SM instability occurring at  $F=0.5$  ML/s is shown in Fig. 1(a). The in-phase SM forms a typical surface ripple structure, which resembles the experimental morphology in MBE growth on Cu(100) vicinal surfaces.<sup>16</sup> As illustrated in Fig. 3(a), the characteristic scaling for the surface roughening rate is 0.67 for the in-phase SM instability mode. When  $F$  reduces to 0.02 ML/s, the initial step fluctuation returns to the stable step-flow, as shown in Fig. 1(b). Comparison of Figs. 1(a) and 1(b) confirms that the ES-barrier-driven SM occurs for large  $F$  but vanishes for small  $F$  when the stress is absent.

The step instability is simulated with the EMMI term incorporated for the case of the stress. For  $F=0.02$  ML/s, the step instability first undergoes out-of-phase SM, then evolves into SB eventually, as shown in Fig. 1(c). This result is consistent with the prediction of the linear stability analysis for crossover from undulation to SB in the case of the initial step separation of the vicinal substrate under stress below the critical value of the intermediate state.<sup>9</sup> As shown in Fig. 3(a), the characteristic scaling value of the surface roughening rate is 0.33 for the SB, less than that for the ES-barrier-driven SM.

When both ES barrier and EMMI are considered in the simulation for  $F=0.02$  ML/s, we obtain a bunching-

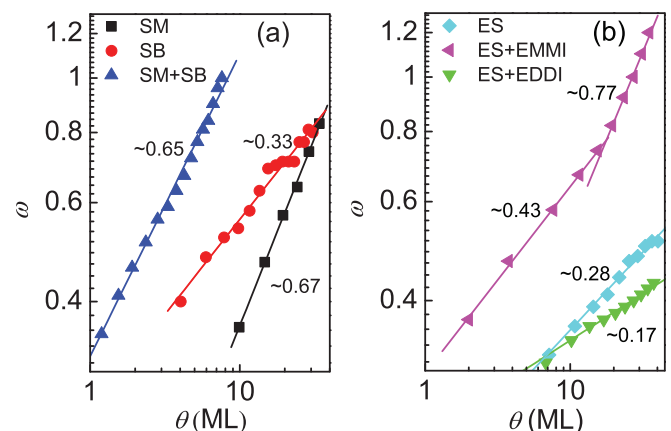


FIG. 3. (Color online) Surface roughness  $w$  versus deposition coverage  $\theta$  obtained for (a) SM, SB, and simultaneous SM and SB instability modes and (b) anisotropy-directed in-phase SM instability mode with EMMI and EDDI terms considered or not.

meandering morphology, as shown in Fig. 1(d). The characteristic scaling law of the surface roughening rate is 0.65, being very close to that for ES-barrier-driven SM instability. The results indicate that the ES barrier can drive meandering instability even for small  $F$  when the stress is present. The possible reason could be that EMMI modifies step stiffness, which decreases the  $F$  threshold for step meandering. In the previous linear stability analysis studies, competing step instabilities, such as between undulations and bunching on the vicinal surface under stress<sup>9</sup> and between ES barrier dominant and elastic interaction dominant instabilities in more complex cases,<sup>10</sup> are divided by a critical value  $l^*$  of the initial step separation of the vicinal substrate. It is known that  $l^*$  is a function of factors such as diffusion rate, step impermeability, step formation energy, stress magnitude, and deposition rate. The ES-barrier-driven SM instability is regarded as one kinetic instability that is supposed to vanish at low  $F$ . However, our results indicate that the ES-barrier-driven SM instability might remain prominent even for low  $F$  in the case of the stress due to interplay of ES barrier and EMMI. Our results emphasize that  $l^*$  is dependent on values of  $F$  considering dependence of the ES barrier effect on the stress effect under small  $F$ , which causes enrichment of the ES-driven instability and enlargement of the undulation or ES-barrier-dominant regimes in the related parameter spaces (for example, Fig. 3 in Ref. 9 or Fig. 8(b) in Ref. 10). The consequence is less  $l^*$  when  $F$  is small.

As discussed in Refs. 1 and 17, a strain field of pre-buried dislocations can change the energy distribution of overlayers, which provides possibility to assume a spatial-dependent magnitude distribution of magnitude of the force monopoles. Here, we define  $P=1.5$  in two thin zones of width  $10 \Delta x$  and  $P=0.5$  in other areas (hereafter called as high P zone and low P zone). Locally, SB is caused in the high P zones as shown in Figs. 2(a) and 2(b). Further, the meandering instability first starts ahead of the high P zones with the stress-induced-undulation mechanism and subsequently proceeds downstairs in the low P zones with the well known Bales-Zangwill mechanism with the ES barrier, as shown in Fig. 2(b). The stress-induced instability acts as pre-

cursor for the ES-barrier-induced instability. The ordered meandering-bunching pattern shown in Fig. 2(b) suggests that SM and SB instabilities can be assembled based on interplay of ES barrier and elastic interaction. In the additional simulations that the step energy anisotropy is incorporated so that the SM growth occurring under small  $F$  can develop the periodical arrays of the surface ripples as shown for high  $F$  in Fig. 1(a). For such circumstance, the EMMI causes sharp increase of the surface roughness [around  $\theta=20$  ML in Fig. 3(b)], and the EDDI leads to a slower roughening rate [Fig. 3(b)] but accompanied by a decaying meandering structure. The results indicate that EMMI and EDDI are disadvantageous for ordered growth of SM. Therefore, a necessary condition for the regularity of SM in the low P zones is the elastic interaction effects are sufficiently small in such areas.

Y.M.Y., Y.L., and X.G. were supported by Nature Science Foundation of China (Grant No. 10974228), and A.V. was supported by DFG through Vo 899/7.

- <sup>1</sup>J. Stangl, V. Holy, and G. Bauer, *Rev. Mod. Phys.* **76**, 725 (2004).
- <sup>2</sup>C. Misbah, O. Pierre-Louis, and Y. Saito, *Rev. Mod. Phys.* **82**, 981 (2010).
- <sup>3</sup>N. Neel, T. Maroutian, L. Douillard, and H.-J. Ernst, *Phys. Rev. Lett.* **91**, 226103 (2003).
- <sup>4</sup>G. S. Bales and A. Zangwill, *Phys. Rev. B* **41**, 5500 (1990).
- <sup>5</sup>O. Pierre-Louis and C. Misbah, *Phys. Rev. Lett.* **76**, 4761 (1996).
- <sup>6</sup>O. Pierre-Louis, C. Misbah, Y. Saito, J. Krug, and P. Politi, *Phys. Rev. Lett.* **80**, 4221 (1998).
- <sup>7</sup>C. Dupont, P. Nozieres, and J. Villain, *Phys. Rev. Lett.* **74**, 134 (1995).
- <sup>8</sup>S. Paulin, F. Gillet, O. Pierre-Louis, and C. Misbah, *Phys. Rev. Lett.* **86**, 5538 (2001).
- <sup>9</sup>F. Leonard and J. Tersoff, *Appl. Phys. Lett.* **83**, 72 (2003).
- <sup>10</sup>D. H. Yeon, P. R. Cha, J. S. Lowengrub, A. Voigt, and K. Thornton, *Phys. Rev. E* **76**, 011601 (2007).
- <sup>11</sup>Y. M. Yu and B. G. Liu, *Phys. Rev. E* **70**, 205414 (2004).
- <sup>12</sup>Y. M. Yu and B. G. Liu, *Phys. Rev. B* **73**, 035416 (2006).
- <sup>13</sup>D. H. Yeon, P. R. Cha, S. I. Chung, and J. K. Yoon, *Met. Mater. Int.* **9**, 67 (2003).
- <sup>14</sup>L. Proville, *Phys. Rev. B* **64**, 165406 (2001).
- <sup>15</sup>W. Lu and Z. Suo, *Phys. Rev. B* **65**, 205418 (2002).
- <sup>16</sup>T. Maroutian, L. Douillard, and H. J. Ernst, *Phys. Rev. B* **64**, 165401 (2001).
- <sup>17</sup>E. Pan, M. Sun, P. W. Chung, and R. Zhu, *Appl. Phys. Lett.* **91**, 193110 (2007).